Journal of Magnetic Resonance **137,** 138–143 (1999)
Article ID jmre.1998.1664, available online at http://www.idealibrary.com on IDEAL®

Resolution Enhancement in ^{13}C and ^{15}N Magic-Angle Turning Experiments with TPPM Decoupling

Gary McGeorge, D. W. Alderman, and David M. Grant[1]

Department of Chemistry, University of Utah, Salt Lake City, Utah 84112-0850, USA

Received July 23, 1998; revised October 15, 1998

Many solid-state spectra have been shown to have problems related to the poor proton decoupling of carbon nuclei in methylene groups under conditions of slow magic-angle turning. Two-pulse phase-modulation (TPPM) decoupling during the 2D PHORMAT chemical shift separation experiment is shown to be more effective in comparison to that obtainable at much higher spin rates using conventional CW decoupling. TPPM decoupling can also alleviate similar inadequacies when observing the ^{15}N nucleus, particularly with NH_2 groups. This is demonstrated in the ^{15}N resonances of fully labeled L-arginine hydrochloride, where a line narrowing of about a factor of two was observed at moderate rotation rates. This significant advantage was also obtained at turning frequencies as low as 500 Hz.

INTRODUCTION

Solid-state NMR spectra of dilute nuclei in organic molecules are broadened by chemical shift anisotropy (CSA) and heteronuclear dipolar couplings to protons (*1*). Typically, these interactions are counteracted with high-speed magic-angle spinning (MAS) in conjunction with continuous wave (CW) proton decoupling. As the optimum decoupler frequency depends upon the proton resonance frequencies, it is often difficult to simultaneously decouple protons with different chemical shifts (*2, 3*). This problem is aggravated at higher fields since the broadening increases nonlinearly with the frequency offset. VanderHart and Campbell discussed the nature of CW proton decoupling of the methylene carbons within linear polyethylene, at various rotation frequencies, decoupler frequencies, and amplitudes, and also B_0 (*4*).

Bennett *et al.* (*5*) and Tekely *et al.* (*3*) improved solid-state decoupling by phase modulating the decoupler radio frequency (RF) field to reduce the linewidths of protonated carbons, while Gan and R. R. Ernst (*6*) suggested a combined frequency and phase modulation of the decoupler. Bennett showed that all lines were more intense as a result of the periodic phase changes. M. Ernst *et al.* (*7*) attributed this increased intensity to a reduction of the amplitude of decoupling sidebands under phase-modulated decoupling. Bennett and Tekely both found that the linewidths were largely independent of sample rotation frequency.

The effectiveness of decoupling as a function of rotation frequency is important because lower frequencies are often utilized to retain the CSA information. At moderate rotation rates (~1 kHz) the principal values of the CSA tensor can be found by careful analysis of spinning-sideband intensities (*8, 9*). Two-dimensional magic-angle turning (MAT) experiments (*10–13*) employ very low rotation frequencies (down to 30 Hz) to exhibit nearly static powder patterns in their acquisition dimension. At these low frequencies it becomes especially difficult to effectively decouple CH_2 protons using CW RF at moderate power levels. An example was presented by Hu *et al.* (*11*) in the PHORMAT spectrum of methyl-α-D-glucopyranoside (MADG), wherein the line from the CH_2 carbon in the projection of the PHORMAT spectrum was significantly broader than it was in the accompanying high-frequency MAS spectrum.

Another reason for studying linewidth as a function of rotation frequency arises from the TIGER processing (*14, 15*) scheme used to reduce the data collection time for the PHORMAT experiment. TIGER processing requires a high quality one-dimensional "guide" spectrum that represents the evolution dimension of the two-dimensional data. The guide spectrum typically is obtained at moderately high rotation frequencies, while the PHORMAT data are obtained at 30 Hz. Consequently, if the linewidth changes with rotation frequency, the guide spectrum will not faithfully represent the evolution dimension response function. The suggestion that TPPM decoupling reduces the linewidth's rotation-frequency dependence thus has especially important implications for TIGER processed PHORMAT datasets.

The behavior of proton decoupling under slow spinning conditions for ^{15}N is also of great interest. This is a consequence of the fact that the protonated nitrogen groups studied here exhibit narrow-span chemical shift tensors. To obtain the ^{15}N CSA data from these narrow bands one must spin relatively slowly to retain enough sideband information to determine accurately the principal values for such systems.

This paper presents a slow-turning ^{13}C PHORMAT spectrum taken at 30 Hz and a ^{15}N pseudo-2D sideband suppression

[1] To whom correspondence should be addressed. Fax: (801) 581-8433; E-mail: grant@chemistry.utah.edu.

1090-7807/99 $30.00

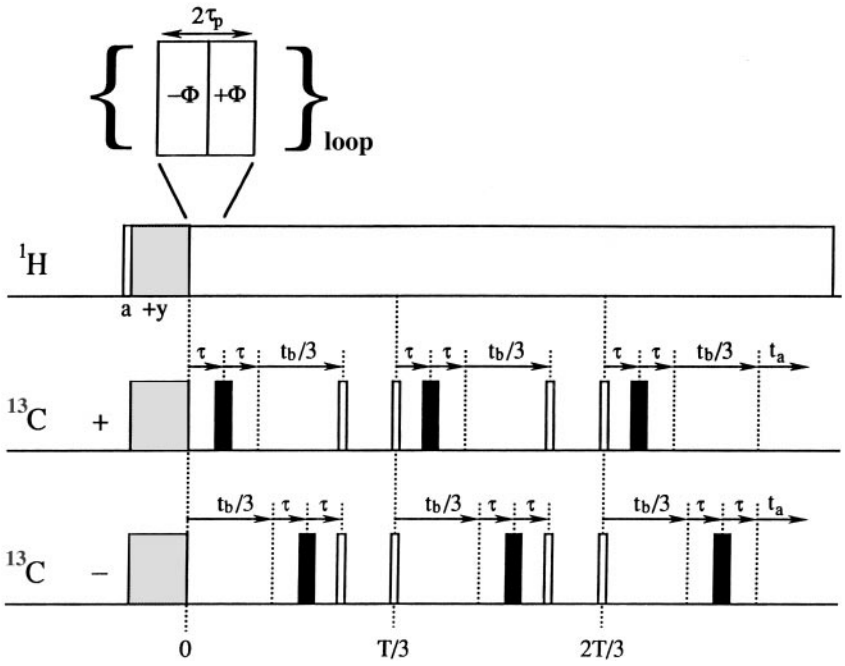

FIG. 1. Pulse sequence used in the PHORMAT experiment with the inclusion of the TPPM decoupling scheme. A 2ϕ total phase-modulation angle of the decoupler is employed, alternating between $+\phi$ and $-\phi$. The cycle time for the phase modulation process is $2\tau_p$.

(P2DSS) (*16*) spectrum taken at 433 Hz that shows how resolution can be significantly improved with the two-pulse phase modulation (TPPM) sequence proposed by Bennett *et al.* (*5*). To obtain these results it was necessary to understand, at least experimentally, how to apply the TPPM pulse sequence at various rotation frequencies.

EXPERIMENTAL

High-resolution ^{13}C and ^{15}N MAS spectra were obtained at 100.2 MHz and 40.55 MHz on a Chemagnetics CMX400 spectrometer using two PENCIL double resonance probes: first, a 7.5-mm probe that delivers a decoupling field equivalent to a nutation frequency of 63 kHz, and second, a 9.5-mm probe capable of 50-kHz decoupling fields. All experiments used cross-polarization with the Hartmann–Hahn match established in adamantane. The magnet was shimmed on adamantane until a linewidth of less than 3 Hz was realized. With the narrow isotropic lines encountered herein, it is imperative that the magic angle be adjusted accurately on the analytical sample as the usual KBr method is not sufficiently sensitive. Extraordinary care was also given to the removal and insertion of samples after establishing the magic angle. The TPPM decoupler frequency must be carefully optimized to avoid broadening the resonances significantly. All ^{13}C shifts were referenced to the high-frequency line of adamantane at 38.56 ppm, and the ^{15}N shifts to the nitrate line of ammonium nitrate at -5.1 ppm.

The PHORMAT experiment used here has been discussed thoroughly, both experimentally and theoretically, by Hu *et al.* (*11*). The PHORMAT/TPPM sequence used in this study on methyl-α-D-glucopyranoside is given in Fig. 1. On the Chemagnetics spectrometer, it is possible to establish independent pulse timing in the observe and decouple channels independently by invoking asynchronous operation of the pulse programmer. Asynchronous operation is necessary in order to produce the TPPM decoupling sequence while retaining the very accurate synchronization of the ^{13}C pulses to the rotor position as described in Ref. *11*. Hence, after the cross-polarization period the carbon and proton channels were operated independently, allowing TPPM decoupling during the evolution period. This timing control is essential to obtain the maximum resolution possible. After the acquisition period the two pulse-programmer channels were returned to synchronous mode. The decoupler interruptions present in the original PHORMAT sequence (*11*) were not included in the TPPM decoupled sequence used here.

The pseudo-2D spinning sideband suppression (P2DSS) method developed by Gan (*16*) was used to obtain sideband-free ^{15}N spectra of enriched L-arginine hydrochloride (*vide infra*). The P2DSS technique involves the collection of a 5π dataset (*12*) with the acquisition dimension sampled synchronously with the rotor. All pulses in the ^{15}N channel of the sequence were synchronized with the rotor position, while the ^{1}H decoupler channel was run asynchronously as described above. The acquisition dimension was sampled every rotor period at the peak of the rotor echo, and the evolution dimension was sampled eight times evenly within one rotor period.

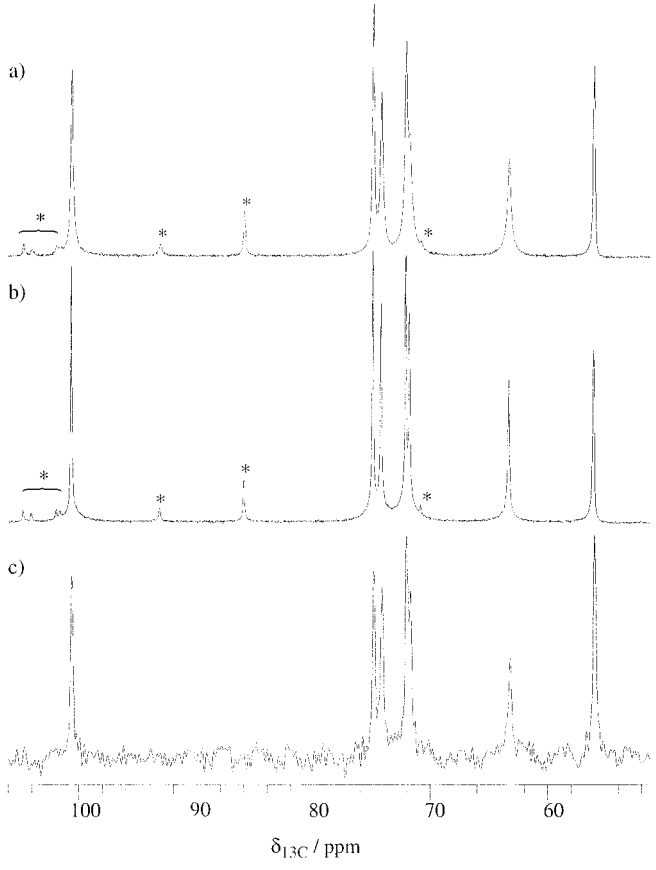

FIG. 2. Comparison of the high-resolution ^{13}C CP/MAS spectra of MADG obtained under various experimental conditions: (a) spinning frequency of 4 kHz with CW decoupling, (b) 4 kHz spinning frequency with TPPM decoupling, (c) evolution dimension projection of the TPPM decoupled PHORMAT spectrum obtained at a spinning frequency of 30 Hz. All decoupling fields correspond to a nutation frequency of 62.5 kHz.

Rearrangement of the 2D 5π data results in a P2DSS 1D dataset with a spectral width eight times the rotor frequency. Spinning stability is essential for good P2DSS results since the spectral widths depend on the instantaneous rotor frequency. Six equally spaced marks on the rotor allowed the spinning stability to be maintained at 433 $\pm$ 0.3 Hz by controlling the drive gas flow rates. A flow constrictor was inserted in the drive gas line to allow for the slow rotation rates.

Methyl-α-D-glucopyranoside was obtained from Aldrich and used as obtained. The enriched L-arginine hydrochloride, obtained from Cambridge Isotopes, was recrystallized from an aqueous solution.

RESULTS AND DISCUSSION

Methyl-α-D-glucopyranoside

Figures 2a and 2b show a comparison of the CW and optimized TPPM decoupled ^{13}C spectra obtained at a spinning frequency of 4 kHz. It is very clear that TPPM decoupling significantly narrows the lines. The 72.5 and 72.1 ppm resonances are not separated with CW decoupling, whereas they are resolved with TPPM decoupling. The linewidths are plotted as a function of spin rate in Fig. 3, for both the TPPM and CW decoupled spectra. In contrast to the CW case, it is evident that the best TPPM results were obtained at slower rotation frequencies. From this observation, it is speculated that extrapolating from 1000 to 30 Hz would significantly reduce the CW decoupling efficiency, whereas the resonances would continue to narrow with TPPM.

All of the TPPM cycle times ($2\tau_p$) of the decoupler modulation were set to $2\pi/\omega_1$. The optimal phase modulation angle

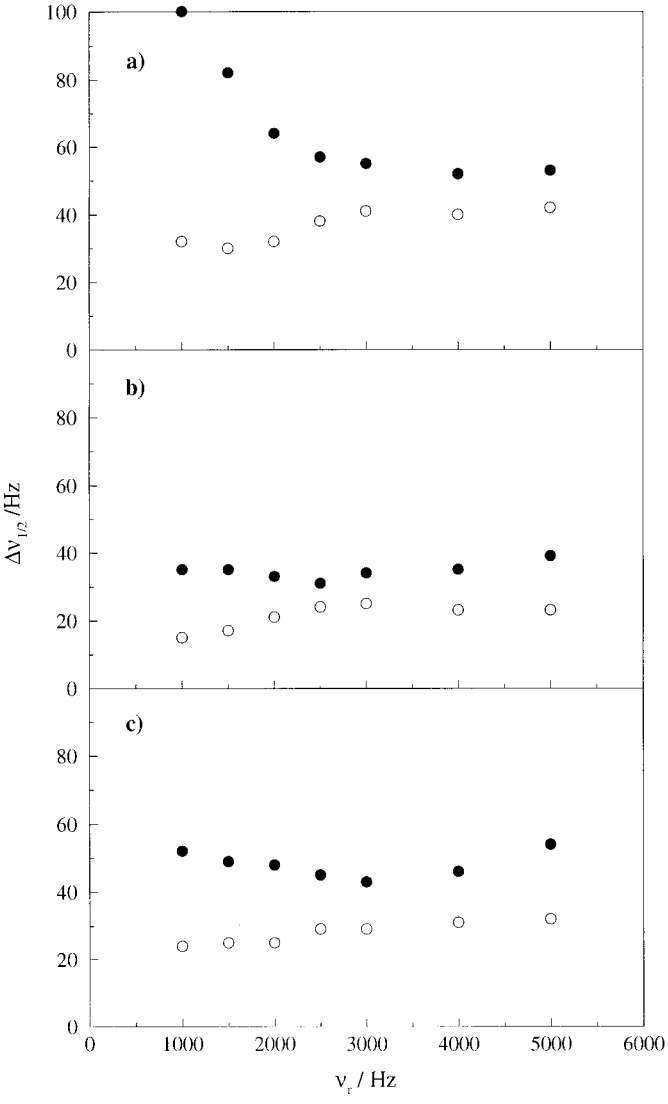

FIG. 3. Carbon-13 linewidths for MADG as a function of MAS spin-frequency for the resonances at (a) 63.3 ppm (CH_2), (b) 72.1 ppm (CH), and (c) 74.2 ppm (CH), under both TPPM (open circles) and CW (solid circles) decoupling schemes. Decoupling fields used in this experiment were ~50 kHz. The linewidths were determined using the deconvolution software within the Chemagnetics Spinsight software and were assumed to be purely Lorentzian, and $\Delta\nu_{1/2}$ is the full width at half maximum.

was found to vary as a function of the rotational rate. At a rotation frequency of 5 kHz the range of angles from $2\Phi = 10°$ to $2\Phi = 22°$ led to performances that were essentially identical. At lower rates the optimum angle increases as the rotation frequency decreases, eventually reaching a plateau value. For MADG the optimum phase angle was found to be about 30° at the lowest frequency. Consequently, a slow MAS spectrum characterizes an approximate optimum phase angle that may be used in the PHORMAT experiment.

Proton-magnetization flip-back (*17*) has typically been utilized in the PHORMAT experiment to increase the signal-to-noise ratio for a given experimental time. Proton-magnetization flip-back is not effective under TPPM decoupling. For flip-back to be effective it is necessary that a significant amount of proton magnetization remain spin-locked along the RF field. Proton spin-locking requires that the magnetization and the decoupler field be colinear at all times, but this is impossible with TPPM's constantly changing decoupler RF phase. This effect was observed in our study of MADG. The loss of the flip-back benefit can lengthen the total experimental time, increasing it by a factor of two or more in some cases.

If the recycle delay is shorter than $\sim 5\ T_1$, the spins are partially saturated. Partial saturation should not be a problem, except that the first transient in the phase cycle, after a longer recycle delay to reload the pulse program, produces a stronger signal. The phase cycle in the two PHORMAT sequences creates linear combinations of successive signals to implement the trigonometric relationships that produce the isotropic shift in the evolution dimension. Additional intensity in the first acquisition reduces the efficiency of the phase cycling and manifests itself as a series of ridges inclined diagonally though the 2D PHORMAT spectrum. To minimize this problem, several dummy pulses (i.e., RF irradiation of the sample, but no data collection) were inserted before the cycle in order to reestablish the partially saturated state.

A portion of the contour plot of the TPPM decoupled ^{13}C PHORMAT spectrum of MADG is shown in Fig. 4. This spectrum exhibits the separation of the powder patterns due to the high resolution developed in the evolution dimension. Figure 2c also compares the projection from the PHORMAT evolution dimension with the CW and TPPM-decoupled MAS spectra. It is encouraging to note that the resolution developed in the evolution dimension of the TPPM-decoupled PHORMAT spectrum is actually better than that from the CW-decoupled spectrum obtained at 4 kHz. To achieve such resolution required the collection of 180 complex data points in the evolution dimension. The principal components obtained for the CSA tensors for MADG with TPPM are presented in Table 1 and compared with the earlier results from PHORMAT data (*11*). Both of these sets of values compare well with those obtained from single-crystal analysis (*11*).

Preliminary results indicate that the linewidth dependence on the decoupler amplitude for TPPM decoupling corresponds to that for CW decoupling (see Ref. *4*: Figs. 7 and 8), except that the TPPM lines are narrower; the difference in linewidths is independent of decoupler amplitude.

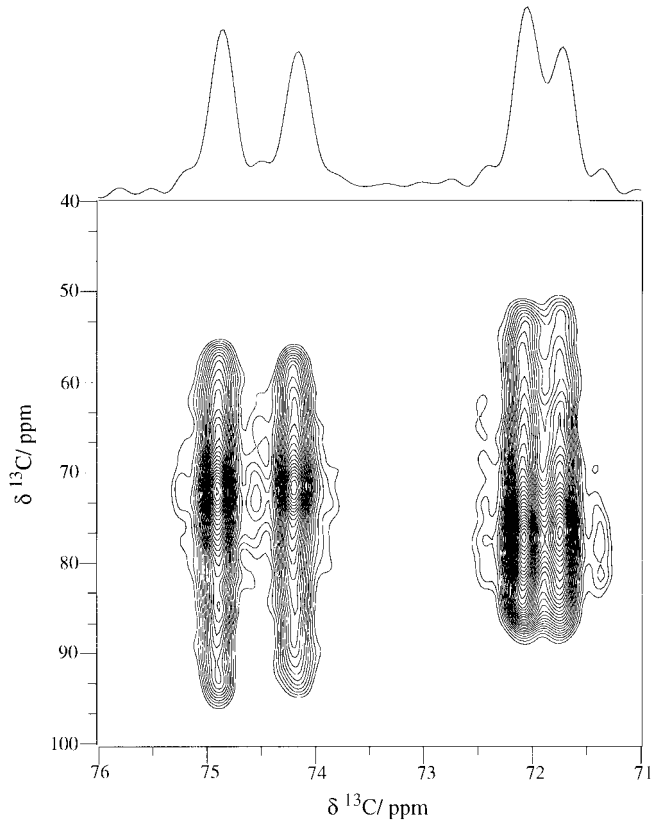

FIG. 4. A portion of the ^{13}C PHORMAT spectrum of MADG. These data were acquired using the sequence shown in Fig. 1, the 7.5-mm probe, a contact time of 3 ms, an echo delay (i.e., τ) of 30 μs, and a recycle delay of 25 s. All radio frequency fields were set to 63 kHz by measuring the null point in a nutation experiment. The PHORMAT sequence does not require a multiple-pulse calibration protocol. The acquisition dimension used a dwell increment of 20 μs with 256 complex points, and the evolution dimension dwell was 181.8 μs with 180 complex points. One dummy pulse was applied prior to starting each increment in the evolution dimension. The evolution projection is shown above to emphasize the resolution obtained.

L-Arginine Hydrochloride

The crystalline solid of L-arginine hydrochloride has four nitrogen atoms per molecule with two independent molecules present in the asymmetric unit. This gives rise to the possibility of observing up to eight ^{15}N isotropic shifts. The ^{15}N TPPM CP/MAS spectrum at 4 kHz (Fig. 5d) shows clearly only seven intense peaks, two for each of the three nitrogens within the guanidino group, but only a single peak of roughly unit intensity, corresponding to the resonance of the NH_3^+ group. (A small shoulder on the NH_3^+ peak, at lower frequency, is also observed. The origin of this anomalous feature is not yet understood.) The narrow spectral lines in Fig. 5 show the advantage of TPPM decoupling at both high (Fig. 5c and 5d) and low (Fig. 5a and 5b) spinning frequencies. The high-speed

TABLE 1
MADG ^{13}C Chemical Shift Tensors[a]

		δ_{11}		δ_{22}		δ_{33}		
	δ_{iso}	PHORMAT[b]	This work	PHORMAT	This work	PHORMAT	This work	Distance[c]
C1	100.7	118.2	118.3	95.2	95.2	89.0	88.5	0.18
C2	72.1	87.7	87.4	78.1	77.5	50.9	51.5	0.33
C3	74.2	94.0	94.1	72.4	72.0	56.7	56.6	0.18
C4	71.8	88.9	87.4	77.2	77.0	49.6	51.0	0.77
C5	74.9	96.0	95.6	72.8	72.8	56.4	56.4	0.16
C6	63.3	89.8	89.3	68.9	68.3	31.6	32.5	0.40
C7	56.1	87.2	86.1	71.2	70.3	10.3	12.0	0.79

[a] Principal components (in ppm from TMS) of the chemical shift tensor as determined by using the banded-matrix treatment of Sethi *et al.* (*8*), which includes the effect of the 30 Hz rotation upon the lineshape.

[b] The PHORMAT results shown are from Hu *et al.* (*11*), from a fitting the full 2D dataset.

[c] The distance between two sets of tensor components is defined by $\text{Distance}^2 = [3(\delta_{11} - \epsilon_{11})^2 + 3(\delta_{22} - \epsilon_{22})^2 + 3(\delta_{33} - \epsilon_{33})^2 + 2(\delta_{11} - \epsilon_{11})(\delta_{22} - \epsilon_{22}) + 2(\delta_{11} - \epsilon_{11})(\delta_{33} - \epsilon_{33}) + 2(\delta_{22} - \epsilon_{22})(\delta_{33} - \epsilon_{33})]/15$, where δ_{ii} are the principal components of one tensor and ϵ_{ii} are the principal components of the other tensor (*18*).

spectra were obtained with standard a CP/MAS sequence, while the slow-spinning were collected using the P2DSS method. Except for the NH_3^+ resonance, the corresponding CW-decoupled lines are approximately twice as wide. TPPM becomes significantly better when the NH dipolar interaction is decoupled at lower rotation rates. The more consistently narrow linewidth of the NH_3^+ lines is presumably due to stochastic torsional rotations about the C–N bond.

The P2DSS protocol contains a fixed-time evolution period of exactly one rotor cycle and results in an exponential loss of magnetization related to the linewidth. The narrower lines have significantly more magnetization at the beginning of the acquisition period, resulting in a higher signal-to-noise ratio, thereby enhancing the benefits of TPPM decoupling. L-Arginine hydrochloride has a very short proton $T_{1\rho}$, and flip-back is therefore ineffective in reducing the recycle time for the data collection even with CW decoupling. Consequently, the experimental-time penalty for using TPPM decoupling is avoided on this sample.

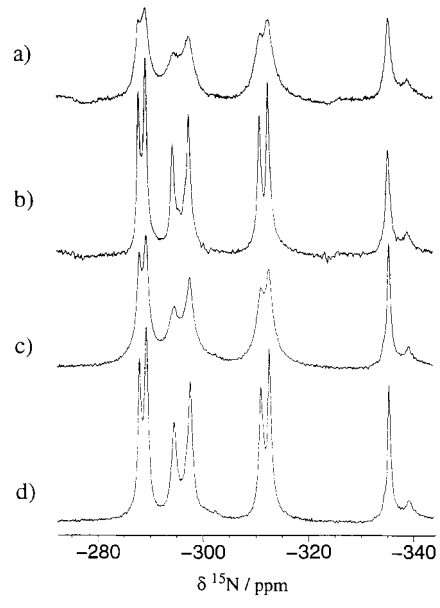

FIG. 5. CP/MAS spectra of 100% ^{15}N enriched L-arginine hydrochloride. The decoupling modulation and spinning frequencies are: (a) CW at 433 Hz; (b) TPPM at 433 Hz; (c) CW at 4 kHz; (d) TPPM at 4 kHz.

CONCLUSIONS

TPPM is a very effective proton decoupling method while observing both ^{13}C and ^{15}N. TPPM is especially useful when the available RF power is insufficient to eliminate completely the homonuclear proton–proton couplings. Further, distinct advantages are clearly observed at lower spinning frequencies. Clearly, much more work has to be carried out to understand the full nature of TPPM decoupling at these slow rotation frequencies.

The effectiveness of TPPM decoupling for observing ^{15}N holds particular promise. The example considered here appears to be quite typical, as line-narrowings with a factor of at least sixfold have been found for a range of nitrogen samples currently being investigated in our laboratory.

ACKNOWLEDGMENTS

This work was supported by the Department of Energy under contract number DE-FG03-94ER1445. We thank D. L. VanderHart for supplying a copy of Ref. *4* prior to publication.

REFERENCES

1. D. L. VanderHart, W. L. Earl, and A. N. Garroway, *J. Magn. Reson.* **44,** 361 (1981).

2. K. Takegoshi and C. A. McDowell, *J. Magn. Reson.* **66,** 14 (1986).
3. P. Tekely, P. Palmas, and D. Canet, *J. Magn. Reson.* **107,** 129 (1994).
4. D. L. VanderHart and G. C. Campbell, *J. Magn. Reson.* **134,** 88 (1998).
5. A. E. Bennett, C. M. Rienstra, M. Auger, K. V. Lakshmi, and R. G. Griffin, *J. Chem. Phys.* **103,** 6951 (1995).
6. Z. Gan and R. R. Ernst, *Solid State NMR* **8,** 153 (1997).
7. M. Ernst, S. Bush, A. C. Kolbert, and A. Pines, *J. Chem. Phys.* **105,** 3387 (1996).
8. N. K. Sethi, D. W. Alderman, and D. M. Grant, *J. Mol. Phys.* **71,** 217 (1990).
9. J. Herzfeld and A. Berger, *J. Chem. Phys.* **73,** 6021 (1980).
10. Z. Gan, *J. Am. Chem. Soc.* **114,** 8307 (1992).
11. J. Z. Hu, W. Wang, F. Liu, M. S. Solum, D. W. Alderman, R. J. Pugmuire, and D. M. Grant, *J. Magn. Reson.* **113,** 210 (1995).
12. J. Z. Hu, D. W. Alderman, C. Ye, R. J. Pugmuire, and D. M. Grant, *J. Magn. Reson.* **105,** 82 (1993).
13. Z. Gan and R. R. Ernst, *J. Magn. Reson.* **123,** 140 (1996).
14. G. McGeorge, J. Z. Hu, C. L. Mayne, D. W. Alderman, R. J. Pugmuire, and D. M. Grant, *J. Magn. Reson.* **129,** 134 (1997).
15. Y. Manassen, G. Navon, and C. T. W. Moonen, *J. Magn. Reson.* **72,** 551 (1987).
16. Z. Gan, *J. Magn. Reson.* **109,** 253 (1994).
17. J. Tegenfeldt and U. Haeberlen, *J. Magn. Reson.* **36,** 453 (1979).
18. D. W. Alderman, M. H. Sherwood, and D. M. Grant, *J. Magn. Reson. A* **101,** 188 (1993).